Elasticity and symmetry of triangular lattice materials

M.L.M. François, Lin Chen, Michel Coret

Elasticity and symmetry of triangular lattice materials

M.L.M. François[a,*], L. Chen[a], M. Coret[b]

[a] *Laboratoire GeM (UMR 6183), Université de Nantes, 2, rue de la Houssinière, 44322 Nantes Cedex 3 (France)*
[b] *Laboratoire GeM (UMR 6183), École Centrale de Nantes, 1 Rue de la Nöe, 44300 Nantes (France)*

Abstract

The elastic tensor of any triangular (2D) lattice material is given with respect to the geometry and the mechanical properties of the links between the nodes. The links can bear central forces (tensional material, for example with hinged joints), momentums (flexural materials) or a combination of the two. The symmetry class of the stiffness tensor is detailed in any case by using the invariants of Forte and Vianello. A distinction is made between the trivial cases where the elasticity symmetry group corresponds to the microstructure's symmetry group and the non-trivial cases in the opposite case. Interesting examples of isotropic auxetic materials (with negative Poisson's ratio) and non-trivial materials with isotropic elasticity but anisotropic fracturation (weak direction) are shown. The proposed set of equations can be used in a engineering process to create a 2D triangular lattice material of the desired elasticity.

Keywords:

*Corresponding author
Email addresses: marc.francois@univ-nantes.fr (M.L.M. François), chenletian47@126.com (L. Chen), michel.coret@ec-nantes.fr (M. Coret)

anisotropic, lattice material, trusses, symmetric, elasticity, invariant, microstructural

1. Introduction

Trusses have been known for their mechanical performances for centuries. Recent progresses in manufacturing (such as 3D printers) have made possible to generate lattice materials for which the truss microstructure is small with respect to the overall structure size. This allows the creation of a wide range of materials in terms of mass volume, strength and rigidity, as is evident in Ashby's charts (Fleck et al., 2010). Furthermore it is also possible to design such materials with respect to optimized anisotropy (Jibawy et al., 2011).

For the sake of simplicity we chose to study the simplest case of triangular lattice. However the methodology should easily be generalized to other lattice patterns, even if it is not obvious that the change of pattern would lead to analytical formulae as it is the case for triangles. The links (beams) between the nodes of the lattice material can transmit forces and/or momentums. From a theoretical point of view we shall refer respectively to tensional and flexural materials. From a technological point of view, pinned joints transmit only forces and solid joints transmit both forces and momentums. The beams can be modelled with various degrees of refinement (Euler Bernoulli, Timoshenko...) however, in the linear domain, each model leads to some tensional and flexural stiffnesses thus to a tensional and flexural spring model. The simplest Euler-Bernoulli's case is shown (Eq. 4) as an example. For simple beam sections, the beam theory shows that the tensional behavior remains predominant. We recall a type of flexible joint where flexural behavior is

predominant.

Whenever it is possible to analytically calculate the forces or momentums in every bar (classical Ritter or Cremona methods) it is generally highly helpful to consider homogenized behavior. Homogenization theory (Bornert et al., 2002) makes a link between microstructural characteristics and the chosen macroscopic kinematic. In this article the retained kinematics is the linear elasticity which is relevant in the case of large structures with respect to the cell size, small strains and small strain gradients. This excludes for example the case of cracking or structures with an average number of cells which require richer kinematics such as micropolar elasticity (Lakes, 1986; Dos Reis and Ganghoffer, 2012) or gradient elasticty (Auffray et al., 2009). With the above hypothesis, the Cauchy-Born rule (Born and Huang, 1954), which states that each truss node displacement is submitted to the macroscopic kinematic field (Le Dret and Raoult, 2011; Dirrenberger et al., 2013), applies and leads to many simplifications. The precision of the retained homogenization process upon the respect of above hypotheses and is discussed in relevant literature (Bornert et al., 2002; Duy-Khanh, 2011).

One of the leading mechanical properties is the symmetry class of the stiffness tensor. These classes have been recently identified in 2D (Blinowski et al., 1996) and in 3D (Forte and Vianello, 1996). For 2D stiffness tensors a set of invariants separates the symmetry classes (Vianello, 1997; De Saxcé and Vallée, 2013; Forte and Vianello, 2014; Auffray and Ropars, 2016) *i.e.* the tensor belongs to a symmetry class if some (polynomial) relationships between these invariants are verified. They are also useful for the measurement of some distance from a stiffness tensor to any symmetry class (François

et al., 1998; De Saxcé and Vallée, 2013). According to Hermann's theorem and Curie's principle, (Wadhawan, 1987; Auffray, 2008) the symmetry group of the elasticity tensor (the consequence) includes the symmetry group of the lattice (the cause): the stiffness tensor cannot be less symmetric than the lattice. We refer to trivial cases when the symmetry groups of the lattice and the tensor are the same or at least when Hermann's theorem can be easily applied (for example a D_3 lattice obviously leads to an isotropic stiffness tensor) and find some interesting non-trivial cases for their original properties. We also detail the well-known case of isotropic elasticity and negative Poisson's ratio (auxetic material) (Milton, 1992, 2002) which has various industrial applications today. Lattice materials can also present some low energy modes in the Kelvin (Thomson) (1856) sense (see also Kelvin (Thomson) (1893); Rychlewski (1984)): a deformation state associated to weak or null stress which makes them at the frontier between materials and mechanisms. Finally, we show a case of an isotropic elastic material with anisotropic (guided) fracturation due to the presence of a weak direction in the material.

Section 2 of this article shows the study of an unique cell. The stiffness tensor is deducted from the homogenization process in section 3 in both cases of the tensile and flexural materials. The symmetry groups and invariants of the stiffness tensors are recalled in section 4. Tensional, flexural and combined tensional and flexural materials are studied for each symmetry class through sketch examples respectively in sections 5, 6 and 7. The necessary conditions on the lattice stiffnesses and geometry for the elasticity tensor to belong to a symmetry class are given. In any relevant case, both trivial and non-trivial cases are studied. As shown by Cauchy (1913), the stiffness

tensors of tensional materials have the full index symmetry (Vannucci and Desmorat, 2016). The flexural lattice material is shown to have a null dilatational mode (in the Kelvin sense), to belong only to the tetragonal or isotropic classes and to have Kelvin elasticity (without the full index symmetry). Particular behavior of flexural and tensile lattice materials, such as auxetic materials (with negative Poisson's ratio) and degenerated materials (with a weak Kelvin mode) are shown. Special attention is payed to a non-trivial isotropic case which presents a weak direction inducing an anisotropic (orientated) fracturation process.

2. The triangular lattice deformation

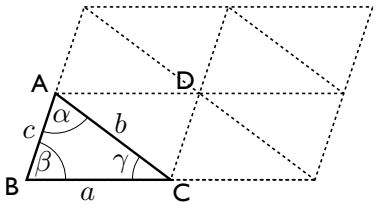

Figure 1: Triangular lattice and triangle parameters at undeformed state

The primitive cell of the lattice is the parallelogram ABCD in Fig. 1. However it is simpler to consider the triangular half cell ABC. The triangular lattice summits (A,B,C) and the angles (α, β, γ) respectively face the bars of lengths (a, b, c) (see Fig. 1). With no restriction we impose $0 < \gamma \leqslant \beta \leqslant \alpha < \pi$, thus the longest length is a (Perrin, 2013). Angles β and γ are retained as independent geometrical parameters. From classical triangle relations one

finds the bounds

$$0 < \beta \leqslant \frac{\pi}{3} \implies 0 < \gamma \leqslant \beta \tag{1}$$

$$\frac{\pi}{3} \leqslant \beta < \frac{\pi}{2} \implies 0 < \gamma \leqslant \pi - 2\beta \tag{2}$$

illustrated in Fig. 2 which also show the loci of particular triangles. From

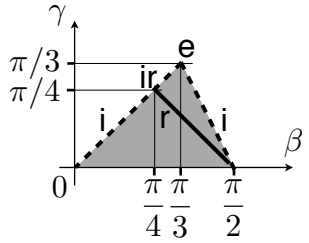

Figure 2: Definition domain of the angles (shaded area) and loci of equilateral (e), isosceles (i), right (r) and right isosceles (ri) triangles.

an homogenization point of view the physical size of the cell is indifferent thus one may set $a = 1$ however a is maintained to indicate the dimension of a length. Under an homogenous deformation field the repetitive lattice deforms in another repetitive one (Fig. 3). As a consequence each node bears identical forces and momentums, rotates through an identical angle θ and each vector $(\mathbf{BC}, \mathbf{CA}, \mathbf{AB})$ rotates respectively through the angles $(\theta_a, \theta_b, \theta_c)$. Supposing linear elastic links the elongation Δa and the relative rotation $\theta - \theta_a$ is respectively proportional to the axial force N_a and the momentum M_a (see Fig. 4)

$$\Delta a = \frac{N_a}{k_a}, \quad \theta - \theta_a = \frac{M_a}{j_a} \tag{3}$$

where, k_a and j_a are respectively the stiffnesses in tension and in flexion. The shear force T_a is given by the statics: $aT_a + 2M_a = 0$ however the shear effects

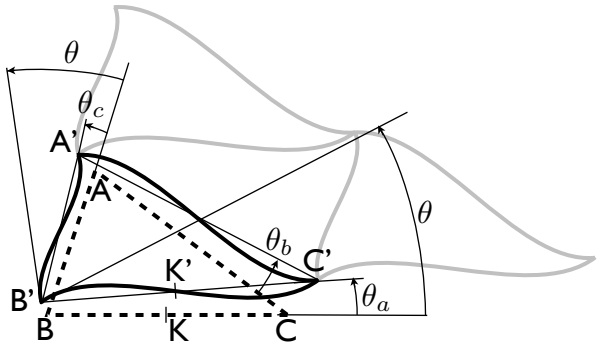

Figure 3: Initial (thick dashed lines) and deformed (thick plain lines) state of a triangular cell and rotation angles

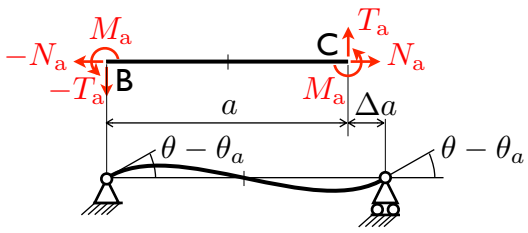

Figure 4: Beam BC. Top: reference geometry and loading. Bottom: kinematics and deformed state

are neglected. In the case of Euler-Bernoulli beams of constant section area s_a, second moment of area i_a and Young's modulus e (of the bulk material) these stiffnesses (in the sense of a spring model) are

$$k_a = \frac{es_a}{a}, \quad j_a = \frac{6ei_a}{a}. \tag{4}$$

Elongations and rotations are related to the node displacements $(\mathbf{u}_\mathrm{B}, \mathbf{u}_\mathrm{C})$ by

$$\Delta a = \mathbf{n}_\mathrm{BC} \cdot (\mathbf{u}_\mathrm{C} - \mathbf{u}_\mathrm{B}), \quad \theta_a = \frac{\mathbf{m}_\mathrm{BC} \cdot (\mathbf{u}_\mathrm{C} - \mathbf{u}_\mathrm{B})}{a} \tag{5}$$

where $(\mathbf{n}_{\rm BC}, \mathbf{m}_{\rm BC})$ are the unit vector respectively proportional and directly orthogonal to $\mathbf{BC}$. Eqs. (3) to (5) are similar for beams b and c. The reference frame $(\mathbf{e}_1, \mathbf{e}_2)$ is defined by $\mathbf{BC} = a\,\mathbf{e}_1$. Denoting the relative displacement components as $u_{\rm BC1} = (\mathbf{u}_{\rm C} - \mathbf{u}_{\rm B}) \cdot \mathbf{e}_1$ *etc.*..., previous equations and momentum equilibrium $M_a + M_b + M_c = 0$ lead to the 7×7 linear system

$$\begin{bmatrix} 1 & 0 & 0 & 0 & 0 & 0 & 0 \\ 0 & 0 & 0 & -1 & 0 & 0 & 1 \\ 0 & -\mathrm{c}_\gamma & 0 & 0 & \mathrm{s}_\beta \mathrm{s}_\gamma / \mathrm{s}_\alpha & 0 & -\mathrm{s}_\beta \mathrm{s}_\gamma / \mathrm{s}_\alpha \\ 0 & \mathrm{s}_\gamma & 0 & 0 & \mathrm{c}_\gamma \mathrm{s}_\beta / \mathrm{s}_\alpha & 0 & -\mathrm{c}_\gamma \mathrm{s}_\beta / \mathrm{s}_\alpha \\ 0 & 0 & -\mathrm{c}_\beta & 0 & 0 & -\mathrm{s}_\beta \mathrm{s}_\gamma / \mathrm{s}_\alpha & \mathrm{s}_\beta \mathrm{s}_\gamma / \mathrm{s}_\alpha \\ 0 & 0 & -\mathrm{s}_\beta & 0 & 0 & \mathrm{c}_\beta \mathrm{s}_\gamma / \mathrm{s}_\alpha & -\mathrm{c}_\beta \mathrm{s}_\gamma / \mathrm{s}_\alpha \\ 0 & 0 & 0 & j_a/a & j_b/a & j_c/a & 0 \end{bmatrix} \cdot \begin{bmatrix} N_a/k_a \\ N_b/k_b \\ N_c/k_c \\ aM_a/j_a \\ aM_b/j_b \\ aM_c/j_c \\ a\theta \end{bmatrix} = \begin{bmatrix} u_{\rm BC1} \\ u_{\rm BC2} \\ u_{\rm CA1} \\ u_{\rm CA2} \\ u_{\rm AB1} \\ u_{\rm AB2} \\ 0 \end{bmatrix} \tag{6}$$

where s_α stands for $\sin\alpha$ and c_α for $\cos\alpha$ *etc.*... The inverse of this system gives

$$\mathsf{F} = \mathsf{K} \cdot \mathsf{U} \tag{7}$$

$$\mathsf{F} = [N_a, N_b, N_c, M_a, M_b, M_c]^{\rm T} \tag{8}$$

$$\mathsf{U} = [u_{\rm BC1}, u_{\rm BC2}, u_{\rm CA1}, u_{\rm CA2}, u_{\rm AB1}, u_{\rm AB2}]^{\rm T} \tag{9}$$

where the detailed expression of the 6×6 matrix K and the value of θ are given by Eqs. (A.1) and (A.2). The elastic energy stored in both the beams

BC, CA and AB is

$$W = \frac{1}{2}\mathsf{F}^T \cdot \mathsf{D} \cdot \mathsf{F} \tag{10}$$

$$\mathsf{D} = \begin{bmatrix} 1/k_a & 0 & 0 & 0 & 0 & 0 \\ 0 & 1/k_b & 0 & 0 & 0 & 0 \\ 0 & 0 & 1/k_c & 0 & 0 & 0 \\ 0 & 0 & 0 & 2/j_a & 0 & 0 \\ 0 & 0 & 0 & 0 & 2/j_b & 0 \\ 0 & 0 & 0 & 0 & 0 & 2/j_c \end{bmatrix} \tag{11}$$

3. The stiffness tensor components

The Cauchy-Born rule (Born and Huang, 1954; Le Dret and Raoult, 2011; Dirrenberger et al., 2013) states that node displacements are given by the homogeneous strain field $\boldsymbol{\varepsilon}$. This strain tensor is projected in a Bechterew's type second order symmetric tensor orthonormal basis (Bechterew, 1926; Walpole, 1984) whose expression with respect to the vector basis $(\mathbf{e}_1, \mathbf{e}_2)$ is

$$\begin{aligned} \mathbf{B}_1 &= \mathbf{e}_1 \otimes \mathbf{e}_1 \\ \mathbf{B}_2 &= \mathbf{e}_2 \otimes \mathbf{e}_2 \\ \mathbf{B}_3 &= \frac{\mathbf{e}_1 \otimes \mathbf{e}_2 + \mathbf{e}_2 \otimes \mathbf{e}_1}{\sqrt{2}} \end{aligned} \tag{12}$$

where $\otimes$ denotes the dyadic (tensor) product. The components $\bar{\varepsilon}_I$ for $I \in \{1, 2, 3\}$ of $\boldsymbol{\varepsilon}$ in the basis $\mathbf{B}_I$ are related to the components ε_{ij} of $\boldsymbol{\varepsilon}$ in the canonical basis as

$$\bar{\varepsilon}_1 = \varepsilon_{11}, \quad \bar{\varepsilon}_2 = \varepsilon_{22}, \quad \bar{\varepsilon}_3 = \sqrt{2}\varepsilon_{12}. \tag{13}$$

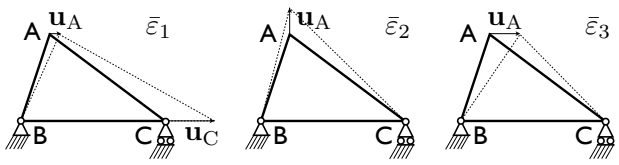

Figure 5: Nodal displacements associated to the elementary strains

The arbitrary rigid body motion is defined by a null displacement of the point B and no rotation of BC (see Fig. 5), giving the nodal displacements by integration of the strain field

$$\begin{aligned}
\mathbf{u}_\mathrm{A} &= c\,(\bar{\varepsilon}_1 \mathrm{c}_\beta + \sqrt{2}\bar{\varepsilon}_3 \mathrm{s}_\beta)\,\mathbf{e}_1 + c\,\bar{\varepsilon}_2 \mathrm{s}_\beta\,\mathbf{e}_2, \\
\mathbf{u}_\mathrm{B} &= \mathbf{0}, \\
\mathbf{u}_\mathrm{C} &= a\,\bar{\varepsilon}_1\,\mathbf{e}_1.
\end{aligned} \tag{14}$$

Thus the relative nodal displacements are

$$\begin{bmatrix} u_{\mathrm{BC}1} \\ u_{\mathrm{BC}2} \\ u_{\mathrm{CA}1} \\ u_{\mathrm{CA}2} \\ u_{\mathrm{AB}1} \\ u_{\mathrm{AB}2} \end{bmatrix} = a \begin{bmatrix} 1 & 0 & 0 \\ 0 & 0 & 0 \\ -\mathrm{s}_\beta \mathrm{c}_\gamma/\mathrm{s}_\alpha & 0 & \sqrt{2}\mathrm{s}_\beta \mathrm{s}_\gamma/\mathrm{s}_\alpha \\ 0 & \mathrm{s}_\beta \mathrm{s}_\gamma/\mathrm{s}_\alpha & 0 \\ -\mathrm{c}_\beta \mathrm{s}_\gamma/\mathrm{s}_\alpha & 0 & -\sqrt{2}\mathrm{s}_\beta \mathrm{s}_\gamma/\mathrm{s}_\alpha \\ 0 & -\mathrm{s}_\beta \mathrm{s}_\gamma/\mathrm{s}_\alpha & 0 \end{bmatrix} \cdot \begin{bmatrix} \bar{\varepsilon}_1 \\ \bar{\varepsilon}_2 \\ \bar{\varepsilon}_3 \end{bmatrix} \tag{15}$$

which is summarized as

$$\mathsf{U} = \mathsf{G} \cdot \mathsf{E} \tag{16}$$

Gathering Eqs. (7), (10) and (16) gives the expression of the truss elastic energy

$$W = \frac{1}{2}[\mathsf{K} \cdot \mathsf{G} \cdot \mathsf{E}]^T \cdot \mathsf{D} \cdot [\mathsf{K} \cdot \mathsf{G} \cdot \mathsf{E}]. \tag{17}$$

Considering that each bar belongs to two adjacent cells, the correspondance between the energy density per unit surface w and W is

$$\begin{aligned} W &= 2Sw \qquad (18)\\ S &= \frac{a^2}{2}\frac{\mathrm{s}_\beta \mathrm{s}_\gamma}{\mathrm{s}_\alpha} \qquad (19)\end{aligned}$$

where S is the area of the cell. The energy density of the homogeneous equivalent material is

$$w = \frac{1}{2}\varepsilon_{ij}C_{ijkl}\varepsilon_{kl} = \frac{1}{2}\bar{\varepsilon}_I \bar{C}_{IJ}\bar{\varepsilon}_J \qquad (20)$$

where $\bar{C}_{IJ}$ are the components of the stiffness tensor $\mathbb{C}$ in the basis $\mathbf{B}_I \otimes \mathbf{B}_J$ Bechterew (1926); Walpole (1984) whose correspondance with the classical components C_{ijkl} in the canonical basis is

$$\begin{aligned} \bar{C}_{11} &= C_{1111}\\ \bar{C}_{22} &= C_{2222}\\ \bar{C}_{12} &= C_{1122}\\ \bar{C}_{13} &= \sqrt{2}C_{1112}\\ \bar{C}_{23} &= \sqrt{2}C_{2212}\\ \bar{C}_{33} &= 2C_{1212} \qquad (21)\end{aligned}$$

From above the stiffness tensor components are obtained by derivation of w with respect to the strain components

$$\begin{aligned} \bar{C}_{IJ} &= \frac{\partial^2 w}{\partial\bar{\varepsilon}_I \partial\bar{\varepsilon}_J}\\ &= \frac{1}{2S}\left[\mathsf{K}\cdot\mathsf{G}\cdot\frac{\partial \mathsf{E}}{\partial \varepsilon_I}\right]^T \cdot \mathsf{D}\cdot\left[\mathsf{K}\cdot\mathsf{G}\cdot\frac{\partial \mathsf{E}}{\partial \varepsilon_J}\right]\\ \bar{\mathsf{C}} &= \frac{1}{2S}\mathsf{G}^T\cdot\mathsf{K}^T\cdot\mathsf{D}\cdot\mathsf{K}\cdot\mathsf{G} \qquad (22)\end{aligned}$$

where $\bar{\mathsf{C}}$ stands for the 3×3 $\bar{C}_{IJ}$ components matrix. The separate role of the stiffnesses in tension (k_a, k_b, k_c) and in flexion (j_a, j_b, j_c) in matrix K and D allow one to establish a partition

$$\mathbb{C} = \mathbb{C}^{\mathrm{t}} + \mathbb{C}^{\mathrm{f}}. \tag{23}$$

in the tensional part $\mathbb{C}^{\mathrm{t}}$ and the flexural part $\mathbb{C}^{\mathrm{f}}$. From Eq. (22) and previous results one finds

$$\begin{aligned}
\begin{bmatrix} \bar{C}^{\mathrm{t}}_{11} \\ \bar{C}^{\mathrm{t}}_{22} \\ \bar{C}^{\mathrm{t}}_{12} \\ \bar{C}^{\mathrm{t}}_{13}/\sqrt{2} \\ \bar{C}^{\mathrm{t}}_{23}/\sqrt{2} \end{bmatrix} &= \frac{1}{\mathrm{s}_\alpha \mathrm{s}_\beta \mathrm{s}_\gamma} \begin{bmatrix} 1 & \mathrm{c}_\gamma^4 & \mathrm{c}_\beta^4 \\ 0 & \mathrm{s}_\gamma^4 & \mathrm{s}_\beta^4 \\ 0 & \mathrm{s}_\gamma^2 \mathrm{c}_\gamma^2 & \mathrm{s}_\beta^2 \mathrm{c}_\beta^2 \\ 0 & -\mathrm{s}_\gamma \mathrm{c}_\gamma^3 & \mathrm{s}_\beta \mathrm{c}_\beta^3 \\ 0 & -\mathrm{s}_\gamma^3 \mathrm{c}_\gamma & \mathrm{s}_\beta^3 \mathrm{c}_\beta \end{bmatrix} \cdot \begin{bmatrix} k_a \mathrm{s}_\alpha^2 \\ k_b \mathrm{s}_\beta^2 \\ k_c \mathrm{s}_\gamma^2 \end{bmatrix} \\
\bar{C}^{\mathrm{t}}_{33} &= 2\bar{C}^{\mathrm{t}}_{12}
\end{aligned} \tag{24}$$

for the tensional part, where the last equation corresponds to the Cauchy (1913) invariance to any index permutation $C^{\mathrm{t}}_{1122} = C^{\mathrm{t}}_{1212}$ which exists as soon as the nodes a related by central forces (no momentum) as is the case for the tensional truss. One remarks that the present case is a sub-case of Cauchy materials for which the nodes interact not only with their nearest

neighbors. Again from Eq. (22) one finds for the flexural part

$$\begin{bmatrix} \bar{C}^{\mathrm{f}}_{11} \\ \bar{C}^{\mathrm{f}}_{13}/\sqrt{2} \\ \bar{C}^{\mathrm{f}}_{33}/2 \end{bmatrix} = \frac{1}{JS} \begin{bmatrix} (\mathrm{s}_\beta \mathrm{c}_\beta + \mathrm{s}_\gamma \mathrm{c}_\gamma)^2 & \mathrm{s}^2_\beta \mathrm{c}^2_\beta & \mathrm{s}^2_\gamma \mathrm{c}^2_\gamma \\ (\mathrm{s}_\beta \mathrm{c}_\beta + \mathrm{s}_\gamma \mathrm{c}_\gamma)(\mathrm{s}^2_\beta - \mathrm{s}^2_\gamma) & \mathrm{s}^3_\beta \mathrm{c}_\beta & -\mathrm{s}^3_\gamma \mathrm{c}_\gamma \\ (\mathrm{s}^2_\beta - \mathrm{s}^2_\gamma)^2 & \mathrm{s}^4_\beta & \mathrm{s}^4_\gamma \end{bmatrix} \cdot \begin{bmatrix} j_b j_c \\ j_c j_a \\ j_a j_b \end{bmatrix} \tag{25}$$

$$\begin{aligned} \bar{C}^{\mathrm{f}}_{22} &= \bar{C}^{\mathrm{f}}_{11} \\ \bar{C}^{\mathrm{f}}_{12} &= -\bar{C}^{\mathrm{f}}_{11} \\ \bar{C}^{\mathrm{f}}_{23} &= -\bar{C}^{\mathrm{f}}_{13} \end{aligned} \tag{26}$$

where $J = j_a + j_b + j_c$. In general $\mathbb{C}^{\mathrm{f}}$ does not have Cauchy symmetry. Lord Kelvin [1856] proposed that any stiffness tensor has three eigentensors in 2D (and 6 in 3D) which correspond to the cases when the stress and strain tensors are proportional. The proportionality factors are referred to as the Kelvin moduli. Rychlewski [1985] showed that the eigenstrains and Kelvin moduli are directly obtained from the diagonalisation of the matrix $\bar{\mathsf{C}}$ whose expression in the Bechterew's basis is in this case

$$\mathbb{C}^{\mathrm{f}} = \begin{bmatrix} \bar{C}^{\mathrm{f}}_{11} & -\bar{C}^{\mathrm{f}}_{11} & \bar{C}^{\mathrm{f}}_{13} \\ -\bar{C}^{\mathrm{f}}_{11} & \bar{C}^{\mathrm{f}}_{11} & -\bar{C}^{\mathrm{f}}_{13} \\ \bar{C}^{\mathrm{f}}_{13} & -\bar{C}^{\mathrm{f}}_{13} & \bar{C}^{\mathrm{f}}_{33} \end{bmatrix}_{\mathbf{B}_I \otimes \mathbf{B}_J} \tag{27}$$

One easily finds that any strain proportional to $\mathbf{I}$ (of components $[1, 1, 0]^{\mathrm{T}}$ in the Bechterew basis) corresponds to null stress

$$\mathbb{C}^{\mathrm{f}} : \mathbf{I} = \mathbf{0}. \tag{28}$$

In other words such material opposes no stiffness to a dilation (see Fig. 6), thus it is in between a material and a mechanism. From an engineering

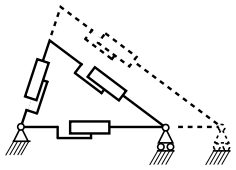

Figure 6: Flexural materials: dilational mode with no rigidity (rectangular boxes represent slide links)

point of view it is necessary to find the mechanical lattice material properties $(a, \alpha, \beta, k_a, k_b, k_c, j_a, j_b, j_c)$ with respect to the six desired independent stiffness tensor components $\bar{C}_{IJ}$. The solution is obviously non unique thus one has to set some values *a priori*. The system (24) (tensile part) is well defined but its inverse is not obvious. The system (25) (flexural part) has six unknowns for three equations (a is hidden in S) however one can verify that the determinant of the matrix of this system is non null (equal to $\mathrm{s}_\alpha^3 \mathrm{s}_\beta^3 \mathrm{s}_\gamma^3$). The determination of the lattice material properties must be numeric and user-aided. However Appendix B lists some linear and quadratic properties which may help.

The simplest realization of a lattice material is to design the links as simple beams of constant section and (in plane) thickness h. Above results and beam theory show that the typical ratio between tensile and flexural components $\bar{C}_{ij}^{\mathrm{t}}/\bar{C}_{ij}^{\mathrm{f}}$ is close to a^2/h^2. The geometry imposes that $h << a$ thus such realization leads to mainly a tensional material. Thus flexural behavior (in particular non Cauchy elasticity) can only be obtained by special designs which allow low tensile rigidity. A technological way to realize frictionless slide links is to use flexible links described in Fig. 7 in which the thin ligaments act as pin joints and lead to a symmetrical frictionless joint with low

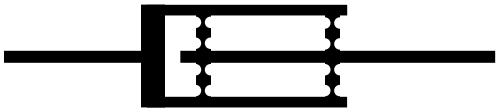

Figure 7: flexible joint with low tensile stiffness

stiffness in tension and a rather simple geometry (Chevalier and Konieczka, 2000).

4. Invariants and symmetry groups of a 2D stiffness tensor

The 2D stiffness tensors only accept four symmetry classes (Verchery, 1982; Vianello, 1997; De Saxcé and Vallée, 2013). They are recalled in Table 1

Table 1: Symmetry classes of the 2D elasticity tensors

Name(s)	Digonal Triclinic	Orthotropic	Tetragonal	Isotropic
Class	Z_2	D_2	D_4	$O(2)$
Generators	$\mathbf{Q}_{(\mathbf{e}_3,\pi)}$	$\mathbf{Q}_{(\mathbf{e}_3,\pi)}$ $\mathbf{Q}_{(\mathbf{e}_1,\pi)}$	$\mathbf{Q}_{(\mathbf{e}_3,\pi/2)}$ $\mathbf{Q}_{(\mathbf{e}_1,\pi)}$	$\mathbf{Q}_{(\mathbf{e}_3,\varphi)}$, $\forall\varphi$ $\mathbf{Q}_{(\mathbf{e}_1,\pi)}$
Sketch example	Z	8	□	◯

in which $\mathbf{Q}(\mathbf{n},\varphi)$ means the rotation of angle φ of axis $\mathbf{n}$. The action of the rotation operator $\mathbf{Q}_{(\mathbf{e}_3,\varphi)}$on $\mathbb{C}$ in the Bechterew's basis is given by De Saxcé and Vallée (2013). Various invariants of 2D stiffness tensors are given in previous references. Among them we retained the five invariants of Vianello

(1997)

$$
\begin{aligned}
I_1 &= \frac{1}{8}(\bar{C}_{11}+\bar{C}_{22}+6\bar{C}_{12}-2\bar{C}_{33}) && (29)\\
I_2 &= \frac{1}{8}(\bar{C}_{11}+\bar{C}_{22}-2\bar{C}_{12}+2\bar{C}_{33}) && (30)\\
I_3 &= \frac{1}{2}(\bar{C}_{11}-\bar{C}_{22})^2+(\bar{C}_{13}+\bar{C}_{23})^2 && (31)\\
I_4 &= \frac{1}{8}[(\bar{C}_{11}+\bar{C}_{22})-2(\bar{C}_{12}+\bar{C}_{33})]^2+(\bar{C}_{13}-\bar{C}_{23})^2 && (32)\\
I_5 &= \frac{\sqrt{2}}{8}\big\{[(\bar{C}_{11}+\bar{C}_{22})-2(\bar{C}_{12}+\bar{C}_{33})]\\
&\quad [(\bar{C}_{11}-\bar{C}_{22})^2-2(\bar{C}_{13}+\bar{C}_{23})^2]\\
&\quad +8(\bar{C}_{13}^2-\bar{C}_{23}^2)(\bar{C}_{11}-\bar{C}_{22})\big\} && (33)
\end{aligned}
$$

where $I_1=\lambda$ and $I_2=\mu$, the Lamé moduli. A sixth invariant I_6 exists but is linked to others by a syzygy and is unhelpful in the present case. One verifies easily that

$$I_3=0 \implies I_5=0 \quad (34)$$

$$I_4=0 \implies I_5=0 \quad (35)$$

Vianello (1997) details the conditions to belong stricly to the symmetry classes. However, since these classes are such that $O(2)\subset D_4\subset D_2\subset Z_2$, we prefer to use the simpler non-strict conditions which are summarized in Fig. 8 and lead, together with Eqs. (34) and (35), to the independent conditions

$$\mathbb{C}\in\mathbb{E}\mathrm{la}(D_2) \iff I_5^2-I_3^2I_4=0 \quad (36)$$

$$\mathbb{C}\in\mathbb{E}\mathrm{la}(D_4) \iff I_3=0 \quad (37)$$

$$\mathbb{C}\in\mathbb{E}\mathrm{la}(O(2)) \iff \begin{cases} I_3=0\\ I_4=0 \end{cases} \quad (38)$$

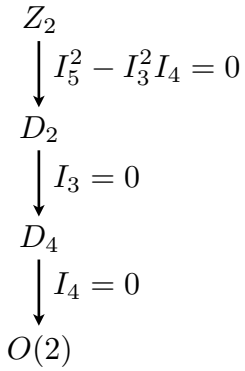

Figure 8: Conditions of appartenance to the 2D symmetry classes of elasticity tensors

where $\mathbb{E}\text{la}(D_2)$ represents the set of stiffness tensors of symmetry class D_2 *etc.*... Some authors also consider the sub-case of orthotropy when $I_4 = 0$ (thus $I_5 = 0$ from Eq. (35)) but $I_3 \neq 0$ called R_0-orthotropy which has interesting theoretical properties (Vannucci, 2002; Auffray, 2017).

We detail hereafter the condition of appartenance to the symmetry classes with respect to the stiffness tensor components. We also recall the expression of the angle φ which defines the natural bases $(\mathbf{e}'_1, \mathbf{e}'_2)$ for which $\mathbf{e}'_1$ is an axis of symmetry. In natural bases the matrix of components $\bar{\mathrm{C}}$ exhibits a maximum of zeros.

For the orthotropic class D_2 the condition of appartenance is, from Eq. (36)

$$\begin{aligned} & (\bar{C}_{12} + \bar{C}_{33} - \bar{C}_{22})(\bar{C}_{11} - \bar{C}_{22})(\bar{C}_{13} + \bar{C}_{23}) \\ = \; & (\bar{C}_{13}^2 - \bar{C}_{23}^2)(\bar{C}_{13} + \bar{C}_{23}) + \bar{C}_{23}(\bar{C}_{11} - \bar{C}_{22})^2 \end{aligned} \tag{39}$$

and the natural basis $\mathbf{e}'_i$ forms an angle φ^{D2} (Auffray and Ropars, 2016) such as

$$\tan(2\varphi^{D2}) = \sqrt{2}\,\frac{\bar{C}_{13} + \bar{C}_{23}}{\bar{C}_{11} - \bar{C}_{22}} \tag{40}$$

with respect to the actual basis $\mathbf{e}_i$. In each of the two natural bases $\bar{C}_{13} = -\bar{C}_{23}$ and, from Eq. (39) $\bar{C}_{23} = 0$ (or $\bar{C}_{11} = \bar{C}_{22}$ but this case induces $I_4 = 0$ thus tetragonal symmetry). In the basis $\mathbf{B}'_I \otimes \mathbf{B}'_J$ associated to $\mathbf{e}'_i$ by Eq. (12) one recovers the well-known expression for an orthotropic tensor in its natural basis

$$\mathbb{C} \in \mathbb{E}\mathrm{la}(D_2) = \left[\begin{array}{ccc} \bar{C}'_{11} & \bar{C}'_{12} & 0 \\ \bar{C}'_{12} & \bar{C}'_{22} & 0 \\ 0 & 0 & \bar{C}'_{33} \end{array}\right]_{\mathbf{B}'_I \otimes \mathbf{B}'_J} \tag{41}$$

For the tetragonal class D_4, the conditions of appartenance (37) gives

$$\left\{\begin{array}{l} \bar{C}_{11} = \bar{C}_{22} \\ \bar{C}_{13} + \bar{C}_{23} = 0 \end{array}\right. \tag{42}$$

and the natural basis $\mathbf{e}''_i$ forms an angle φ^{D4} such as

$$\tan(4\varphi^{D4}) = 2\sqrt{2}\,\frac{\bar{C}_{13}}{\bar{C}_{11} - \bar{C}_{33} - \bar{C}_{12}} \tag{43}$$

with respect to the actual basis $\mathbf{e}_i$. In each of the four natural bases the components of the tetragonal stiffness tensor are of the (also well-known) type

$$\mathbb{C} \in \mathbb{E}\mathrm{la}(D_4) = \left[\begin{array}{ccc} \bar{C}''_{11} & \bar{C}''_{12} & 0 \\ \bar{C}''_{12} & \bar{C}''_{11} & 0 \\ 0 & 0 & \bar{C}''_{33} \end{array}\right]_{\mathbf{B}''_I \otimes \mathbf{B}''_J} \tag{44}$$

The condition (38) of appartenance to the isotropic class $O(2)$ and Eqs. (31) and (32) show that the components of a $O(2)$-invariant stiffness tensor are, in any basis (due to the isotropy):

$$\mathbb{C} \in \mathbb{E}\mathrm{la}(O(2)) = \left[\begin{array}{ccc} \bar{C}_{11} & \bar{C}_{12} & 0 \\ \bar{C}_{12} & \bar{C}_{11} & 0 \\ 0 & 0 & \bar{C}_{11} - \bar{C}_{12} \end{array}\right]_{\mathbf{B}_I \otimes \mathbf{B}_J} \tag{45}$$

5. Tensional lattice materials

In case of tensional lattice material the flexural rigidities are $j_a = j_b = j_c = 0$ and the elasticity tensor is $\mathbb{C} = \mathbb{C}^{\mathrm{t}}$. We show hereafter some representative cases of such materials for each possible case of symmetry class. Each case is illustrated by a drawing of the lattice in which the lines widths of the bars are proportional to their corresponding stiffnesses (k_a, k_b, k_c). Young's modulus

$$E(\mathbf{n}) = \frac{1}{\mathbf{n} \cdot \mathbf{n} \cdot \mathbb{S} \cdot \mathbf{n} \cdot \mathbf{n}} \tag{46}$$

where $\mathbf{n} \in [\mathbf{e}_1, \mathbf{e}_2]$ is a unit vector and $\mathbb{S}$ denotes the inverse of $\mathbb{C}$ (given by $\bar{\mathsf{S}} = \bar{\mathsf{C}}^{-1}$ in the Bechterew basis (Rychlewski, 1984)), is represented in polar plots in order to show the mechanical symmetry. The axes of symmetry are represented by thin dashed lines.

5.1. Digonal case

When no particular relation exists between the stiffness tensor components the elastic tensor belongs to the (lowest) Z_2 symmetry class which is called digonal (or triclinic, a crystallographic name more adapted to 3D).

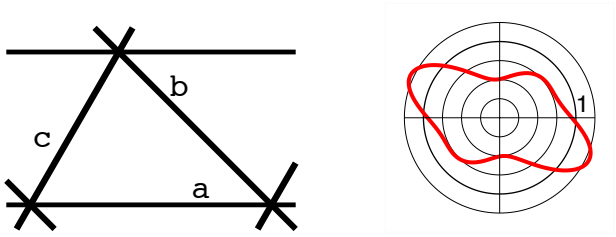

Figure 9: digonal tensional lattice material structure and Young's modulus

Table 2: digonal tensional lattice material characteristics

β	γ	k_a	k_b	k_c
$\pi/3$	$\pi/4$	0.6	0.75	0.8

Table 2 and Fig. 9 show an example of such material. Young's modulus polar plot only exhibits the central symmetry.

5.2. Orthotropic case

The material is orthotropic (of class D_2) if the condition (39) is fulfilled. Together with the Cauchy's condition in Eq. (24) this gives:

$$\bar{C}^{\mathrm{t}}_{12} + \bar{C}^{\mathrm{t}}_{33} - \bar{C}^{\mathrm{t}}_{22} = (\bar{C}^{\mathrm{t}}_{11} - \bar{C}^{\mathrm{t}}_{22})/2 - (\bar{C}^{\mathrm{t}}_{11} + \bar{C}^{\mathrm{t}}_{22} - 6\bar{C}^{\mathrm{t}}_{12})/2 \qquad (47)$$

where each term is related to microstructural properties by Eq. (B.2). An

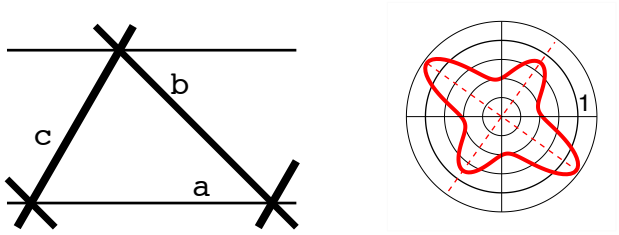

Figure 10: orthotropic tensional lattice material structure and Young's modulus

example of such material is given by Table 3 and Fig. 10. The two orthogonal axes of symmetry of this class are visible on Young's modulus polar plot. They are located by the angle φ^{D2} (Eq. 40).

Table 3: orthotropic tensional lattice material characteristics

β	γ	k_a	k_b	k_c
$\pi/3$	$\pi/4$	0.338	0.833	1

The special case of R_0-orthotropy is fulfilled if $I_4 = 0$. From Eqs. (32) and (24) this corresponds to

$$\begin{bmatrix} \mathrm{s}_\alpha^2 & \mathrm{s}_\beta^2 \mathrm{c}_{4\gamma} & \mathrm{c}_{4\beta} \mathrm{s}_\gamma^2 \\ 0 & \mathrm{s}_\beta \mathrm{c}_\gamma \mathrm{c}_{2\gamma} & -\mathrm{c}_\beta \mathrm{c}_{2\beta} \mathrm{s}_\gamma \end{bmatrix} \cdot \begin{bmatrix} k_a \\ k_b \\ k_c \end{bmatrix} = \begin{bmatrix} 0 \\ 0 \end{bmatrix} \tag{48}$$

Given a set of angles this system defines the ratios between stiffnesses.

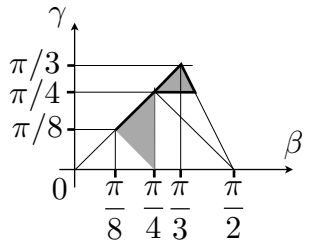

Figure 11: Definition domain of the R_0-orthotropy (shaded area)

Table 4: R_0-orthotropic ($I4 = 0$) tensional lattice material characteristics

β	γ	k_a	k_b	k_c
1	$\pi/3.3$	0.809	0.746	0.65

189

190 Fig. 11 shows the angles for which the R_0-orthotropy can be realized with

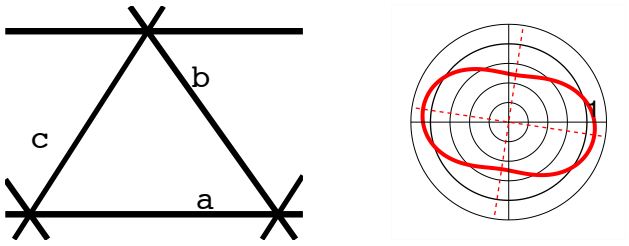

Figure 12: R_0-orthotropic ($I4 = 0$) tensional lattice material structure and Young's modulus

positive stiffnesses (k_a, k_b, k_c). An example of such material is given by Table 4 and Fig. 12. Again the two orthogonal axes of symmetry given by Eq. (40) are visible on Young's modulus polar.

When the symmetry class is already visible on the material structure, this refers to a trivial case (it is not the case in previous examples). For the orthotropic symmetry this requires both $\beta = \gamma$ (isosceles triangle) and $k_b = k_c$. One easily verifies that the obtained stiffness tensor is orthotropic and that $\bar{C}_{13} = \bar{C}_{23} = 0$, thus the actual basis is also a natural one. If furthermore one wants a R_0-orthotropic material, condition (48) gives

$$\frac{k_a}{k_c} = -\frac{2\mathrm{s}_\beta^2 \mathrm{c}_{4\beta}}{\mathrm{s}_\alpha^2} \tag{49}$$

If furthermore one sets $\beta = \gamma = \pi/4$ (isosceles rectangle triangle) this leads to $k_a = k_b = k_c$. This simple way to construct a R_0-orthotropic material is illustrated by Table 5 and Fig. 13 on which the two orthogonal axes of symmetry are visible on both the structure and Young's modulus polar plot.

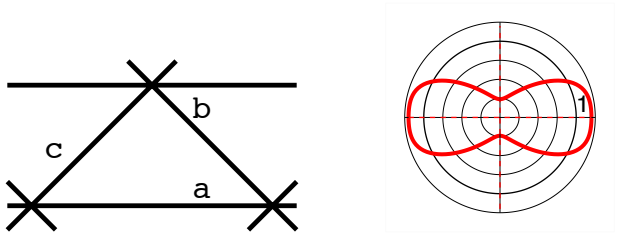

Figure 13: trivial R_0-orthotropic ($I4 = 0$) isosceles tensional lattice material structure and Young's modulus

Table 5: trivial R_0-orthotropic ($I4 = 0$) isosceles tensional lattice material characteristics

β	γ	k_a	k_b	k_c
$\pi/4$	$\pi/4$	0.6	0.6	0.6

5.3. Tetragonal case

The condition (38) to belong to the tetragonal class gives, together with the stiffness tensor expression (24) and Eq. (31)

$$\begin{bmatrix} \mathrm{s}_\alpha^2 & \mathrm{s}_\beta^2\mathrm{c}_{2\gamma} & \mathrm{c}_{2\beta}\mathrm{s}_\gamma^2 \\ 0 & \mathrm{s}_\beta\mathrm{c}_\gamma & -\mathrm{c}_\beta\mathrm{s}_\gamma \end{bmatrix} \cdot \begin{bmatrix} k_a \\ k_b \\ k_c \end{bmatrix} = \begin{bmatrix} 0 \\ 0 \end{bmatrix} \tag{50}$$

Given the angles, this system defines the ratios between the stiffnesses. The angles for which a tetragonal case is possible with positive stiffnesses are shown in Fig. 14. A case of a generic tetragonal truss is given in Table 6 and Fig. 15. The four axes of symmetry which are visible on Young's modulus polar plot are located by φ^{D4} (Eq. 43).

The trivial case is when the structure is obviously tetragonal thus exhibits the four regularly spaced axes of symmetry. This requires $\beta = \gamma = \pi/4$,

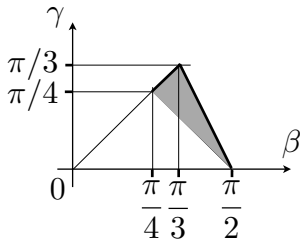

Figure 14: Definition domain of the tetragonal symmetry (shaded area)

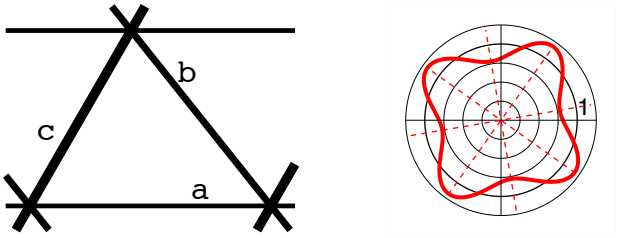

Figure 15: tetragonal tensional lattice material structure and Young's modulus

Table 6: tetragonal tensional lattice material characteristics

β	γ	k_a	k_b	k_c
$\pi/3$	$\pi/3.5$	0.591	0.869	1.2

$k_b = k_c$ and $k_a = 0$. One remarks that the last condition is also imposed by Eq. (50). This corresponds to a degenerated case where the material has a null Young's modulus in any direction except along the bars b and c making such material a four-bar mechanism. It corresponds in some way to a balanced [0-90] (standard designation) composite laminate whose matrix is infinitely weak, *i.e.* a tissue. An example of it is given in Fig. 16 and Table 7.

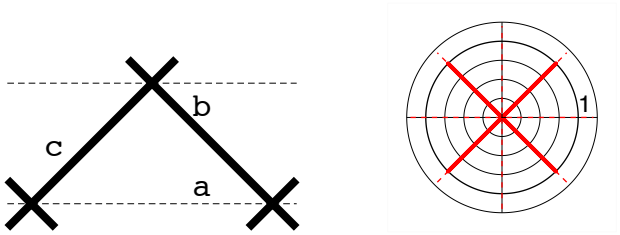

Figure 16: trivial tetragonal tensional lattice material structure and Young's modulus

Table 7: trivial tetragonal tensional lattice material characteristics

β	γ	k_a	k_b	k_c
$\pi/4$	$\pi/4$	0	1	1

5.4. Isotropic case

The condition (38) for isotropy corresponds to both conditions (48) and (50) respectively of R_0-orthotropy and tetragonal class. The solution of this system corresponds to equilateral triangle and equal stiffnesses. Fig. 17 and

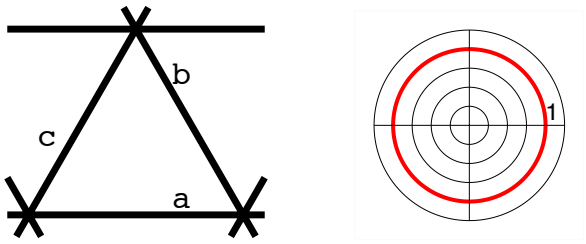

Figure 17: isotropic tensional lattice material structure and Young's modulus

Table 8 show an example of this case (the axis of symmetry are not drawn for clarity). The symmetry class of the structure is obviously D_3 and this case illustrates Hermann's theorem (Wadhawan, 1987; Auffray, 2008) which

Table 8: isotropic tensional lattice material characteristics

β	γ	k_a	k_b	k_c
$\pi/3$	$\pi/3$	0.866	0.866	0.866

states that the symmetry class of the elastic tensor is the lowest possible which includes the one of the structure. The group D_3 cannot be strictly supported by the stiffness tensor (see Table 1) so the elastic tensor symmetry can only be $O(2)$ which is the first (and only one) to include D_3. For this reason, one can also refer to trivial isotropy in this case .

6. Flexural lattice materials

In this section the stiffness tensor $\mathbb{C}^{\mathrm{f}}$ of the sole flexural part of the stiffness tensor is analyzed. This case corresponds to $k_a = k_b = k_c = 0$. One easily verifies from Eq. (27) that $I_3 = 0$ (and $I_5 = 0$) thus $\mathbb{C}^{\mathrm{f}}$ is at least tetragonal. The natural basis for a tetragonal tensor is given by Eq. (43). In such basis $\mathbb{C}^{\mathrm{f}}$ is of the form

$$\mathbb{C}^{\mathrm{f}} = \begin{bmatrix} \bar{C}^{\mathrm{f}}_{11}{}'' & -\bar{C}^{\mathrm{f}}_{11}{}'' & 0 \\ -\bar{C}^{\mathrm{f}}_{11}{}'' & \bar{C}^{\mathrm{f}}_{11}{}'' & 0 \\ 0 & 0 & \bar{C}^{\mathrm{f}}_{33}{}'' \end{bmatrix}_{\mathbf{B}''_I \otimes \mathbf{B}''_J} \tag{51}$$

Obviously this matrix is not inversible thus Young's modulus is undefined. This is in relation with the observation of the null Kelvin modulus associated with the dilational mode by Eq. (28). For this reason we chose to represent the anisotropic behavior thanks to:

$$E'(n) = \mathbf{n} \cdot \mathbf{n} \cdot \mathbb{C} \cdot \mathbf{n} \cdot \mathbf{n} \tag{52}$$

which one may call a pseudo-Young modulus and represents the stiffness of the material under a pure extension of direction $\mathbf{n}$. In every further illustration of sketch examples, the magnitude of the bending stiffnesses (j_a, j_b, j_c) are represented as proportional to the width of a part of a circle (which mimics a flexural spring). To represent the absence of stiffness in tension the beams are drawn with dashed lines.

6.1. Tetragonal case

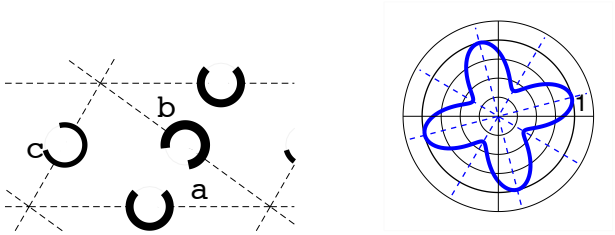

Figure 18: tetragonal flexural lattice material structure and pseudo-Young's modulus

Table 9: tetragonal flexural lattice material characteristics

β	γ	j_a	j_b	j_c
$\pi/3$	$\pi/5$	0.6	0.7	0.4

Table 9 and Fig. 18 show a generic case of such material. The tetragonal behavior is visible on the polar of E' from the four regularly spaced axes of symmetry whose angles φ^{D4} are given by Eq. (43).

The case of trivial tetragonal symmetry requires (similarly to the tensional material in Table 7) $\beta = \gamma = \pi/4$, $j_b = j_c$ and $j_a = 0$. Eq. (25) leads

to $C_{11} = 2j_c/a^2$ and $C_{33} = 0$. The stiffness tensor has a second null Kelvin modulus which is relative to the pure shears proportional to $\mathbf{B}_3$. Such material is also a mechanism with two degrees of freedom. Fig. 19 and Table 10

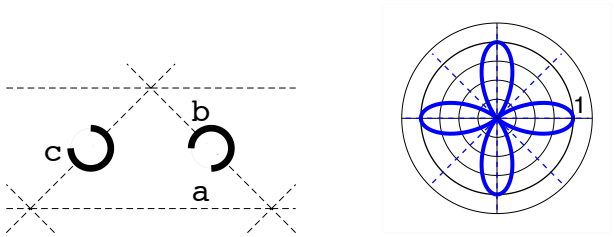

Figure 19: trivial tetragonal flexural lattice material structure and pseudo-Young's modulus

Table 10: trivial tetragonal flexural lattice material characteristics

β	γ	j_a	j_b	j_c
$\pi/4$	$\pi/4$	0	0.5	0.5

show an example of such material.

6.2. Isotropic case

Being at least tetragonal, $\mathbb{C}^{\mathrm{f}}$ can also be isotropic. From conditions of isotropy (38), Eq. (31), (32) and the stiffness tensor components (25) one finds the conditions

$$\frac{j_b}{\tan(\beta)} = \frac{j_c}{\tan(\gamma)} = \frac{j_a}{\tan(\alpha)} \tag{53}$$

for a flexural lattice material to be isotropic. At first we detail the case of trivial isotropy obtained when the microstructure obviously belongs to

the D_3 symmetry class (equilateral triangle and equal stiffnesses) thus the behavior is isotropic from Hermann's theorem (Wadhawan, 1987; Auffray, 2008). Condition (53) leads to $j_a = j_b = j_c$. An example is shown in Fig. 20

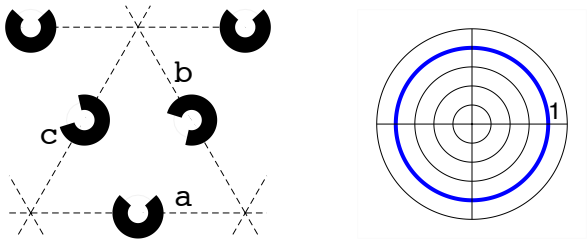

Figure 20: trivial isotropic flexural lattice material structure and pseudo-Young's modulus

Table 11: trivial isotropic flexural lattice material characteristics

β	γ	j_a	j_b	j_c
$\pi/3$	$\pi/3$	1.15	1.15	1.15

and Table 11.

However if the triangle is not equilateral one can create a non trivial isotropic material if the flexural properties (j_a, j_b, j_c) obey the isotropy conditions (53). An example is shown in Fig. 21 and Table 12.

Table 12: non-trivial isotropic flexural lattice material characteristics

β	γ	j_a	j_b	j_c
$\pi/3$	$\pi/5$	1.1	0.2	0.0839

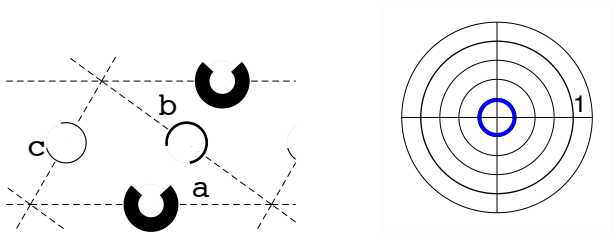

Figure 21: non-trivial isotropic flexural lattice material structure and pseudo-Young's modulus

7. Combined flexural and tensile lattice materials

We address hereafter the general case where the links between nodes have both rigidities in tension (k_a, k_b, k_c) and in flexion (j_a, j_b, j_c). The complete stiffness tensor is given by Eqs. (23), (24) and (25). The number of independent material parameters $(a, \beta, \gamma, k_a, k_b, k_c, j_a, j_b, j_c)$ is larger than the six stiffness tensor independent components (even if the lattice size a has an independent role and must be set at first). Thus there are infinite ways to build a triangular lattice material, given the stiffness tensor. However we shall detail some examples with interesting properties in terms of symmetry or mechanical properties such as auxetic materials (with negative Poisson's ratio) and materials with isotropic elasticity but with orientated fracturation.

7.1. Anisotropic case

Table 13: anisotropic lattice material characteristics

β	γ	k_a	k_b	k_c	j_a	j_b	j_c
$\pi/3$	$\pi/4$	0.4	0.5	0.6	0.04	0.2	0.16

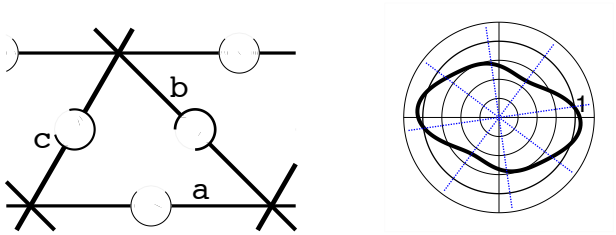

Figure 22: anisotropic lattice material structure and Young's modulus

Table 13 and Fig. 22 show a generic case. Both tensile and flexural parts belong to the lowest symmetry class possible: Z_2 for $\mathbb{C}^{\mathrm{t}}$ and D_4 for $\mathbb{C}^{\mathrm{f}}$ (whose four axes of symmetry are represented by the set of four blue dashed lines on Young's modulus polar plot). The resulting tensor $\mathbb{C}$ inherits from the lowest class, the sole central symmetry Z_2.

7.2. Tetragonal case

The case when $\mathbb{C}^{\mathrm{t}}$ is tetragonal is interesting because even if the four axis of symmetry of $\mathbb{C}^{\mathrm{t}}$ do not coincide with the axes of symmetry of $\mathbb{C}^{\mathrm{f}}$, the final elasticity $\mathbb{C}^{\mathrm{t}} + \mathbb{C}^{\mathrm{f}}$ is also tetragonal (with a third different set of axes of symmetry). This addresses the generic property: the sum of two tetragonal elastic tensors is a tetragonal elastic tensor (even if their axes of symmetry do not coincide). The proof lies in the linearity of the condition (42) related to $I_3 = 0$. A sketch example is shown in Fig. 23 and Table 14. Young's

Table 14: tetragonal lattice material characteristics

β	γ	k_a	k_b	k_c	j_a	j_b	j_c
$\pi/3$	$\pi/3.5$	0.295	0.434	0.6	0.5	0.5	0.25

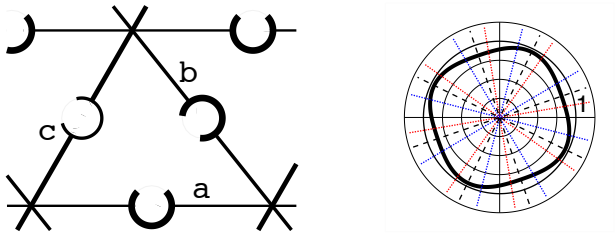

Figure 23: tetragonal lattice material structure and Young's modulus

modulus polar plot exhibits the four axis of symmetry of the tetragonal resulting symmetry (black dashed lines) which do not coincide to the axis of the tensional part (red dashed lines) nor the flexural part (blue dashed lines).

7.3. Trivial (isosceles) isotropic case and auxeticity

We already referred to trivial isotropy which is the case when the microstructure is D_3 invariant (in association with the Hermann's theorem). In the present case this leads to $\alpha = \beta = \gamma = \pi/3$, $k_a = k_b = k_c = k$ and $j_a = j_b = j_c = j$. The form of the isotropic tensor (45) is related to four linear relations between the components thus if both $\mathbb{C}^{\mathrm{t}}$ and $\mathbb{C}^{\mathrm{f}}$ are isotropic tensors, $\mathbb{C}^{\mathrm{t}} + \mathbb{C}^{\mathrm{f}}$ is isotropic too. An example of this case is shown in Fig. 24

Table 15: trivial isotropic lattice material characteristics

β	γ	k_a	k_b	k_c	j_a	j_b	j_c
$\pi/3$	$\pi/3$	0.5	0.5	0.5	0.5	0.5	0.5

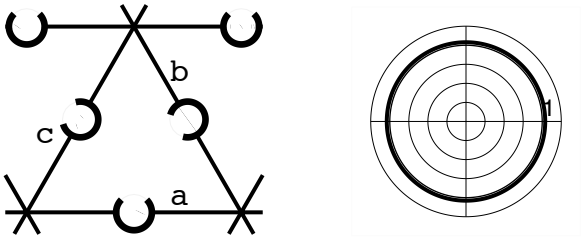

Figure 24: trivial isotropic lattice material structure and Young's modulus

and Table 15. Poisson's ratio generic expression is

$$\nu(\mathbf{n},\mathbf{m}) = -\frac{\mathbf{n}\otimes\mathbf{n} : \mathbb{S} : \mathbf{m}\otimes\mathbf{m}}{\mathbf{n}\otimes\mathbf{n} : \mathbb{S} : \mathbf{n}\otimes\mathbf{n}} \tag{54}$$

where $\mathbf{n}$ is the tensile direction and $\mathbf{m}$ the orthogonal one (for all $\mathbf{n}$ is this isotropic case). More generally, one verifies easily from Eqs. (24) and (25) that

$$E = 2\sqrt{3}\,k\frac{a^2k+2j}{3a^2k+2j} \tag{55}$$

$$\nu = \frac{a^2k-2j}{3a^2k+2j} \tag{56}$$

This leads to the value $\nu = -0.2$ for the example and to the curve in Fig. 25 which shows that Poisson's ratio is negative if $2j > a^2k$, equal to $1/3$ if $j = 0$ (the trivial isotropic tensional material shown in Fig. 17 and Table 8) and equal to -1 if $k = 0$ (the trivial isotropic flexural material shown in Fig. 20 and Table 11) which corresponds to the well-known auxetic material presented by Rothenburg et al. (1991). One easily verifies that for beam of constant rectangular section and of aspect ratio equal to ten, $a^2k/2j = 100$ thus the realization of auxetic triangular lattices require special joints such as the one shown in Fig. 7.

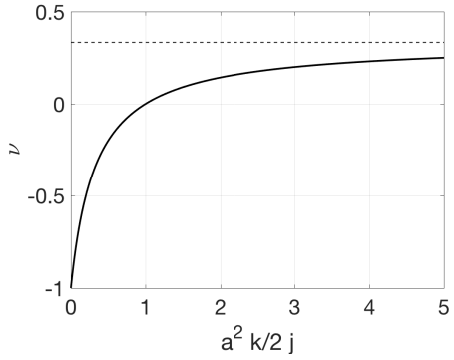

Figure 25: Evolution of Poisson's ratio with respect to the beam properties is case of trivial isotropic material

7.4. Non trivial isotropic case

The isotropy of the tensional lattice material requires an isosceles triangle and equal stiffnesses (Fig. 17) however this is not the case for flexural lattice materials (Fig. 21). We show hereafter an isotropic lattice material composed by the assemblage of a tetragonal tensional part and a tetragonal flexural part whose anisotropy compensate each other. Given a arbitrary geometry (a, β, γ) the unknowns are the six stiffnesses. Two equations are given by the conditions (50) on $\mathbb{C}^t$ to be tetragonal. Another one is given by the angle φ_{D4} which must be common for $\mathbb{C}^t$ and $\mathbb{C}^f$. The last two equations are given by the two relations associated to the condition $(I_4 = 0)$ which remains on the whole tensor to be isotropic (from tetragonal). Finally only one stiffness remains to be user defined.

This process has been used for the example in Fig. 26 and Table 16. The elastic behavior is isotropic but one may think that the fracture behavior will not be isotropic because of the relative weakness of the bars a and b

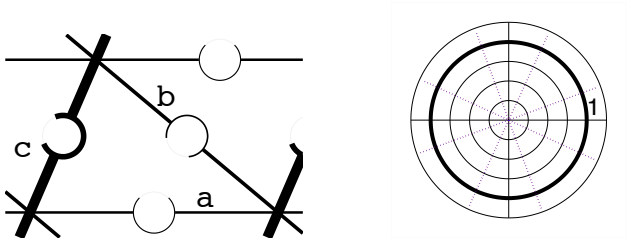

Figure 26: isotropic lattice material structure and Young's modulus

Table 16: isotropic lattice material characteristics

β	γ	k_a	k_b	k_c	j_a	j_b	j_c
$\pi/2.7$	$\pi/4.5$	0.315	0.454	1.25	0.0841	0.123	0.418

(from both flexural and tensional points of view) may lead the fracture to be driven preferentially across the bars of type a and b, *i.e.* parallel to the direction of the bars c. Such a type of behavior may be of interest in the field of structured materials for which the fracture process is begining to interest the community (Fleck et al., 2010; Réthoré et al., 2015). It is also possible to combine weak direction and auxeticity.

8. Conclusion

This article investigates the field of triangular lattice material elasticity and symmetry. Both the stiffness tensor and its symmetry class are given with respect to the lattice properties (angles, tensional and flexural stiffnesses of the links). It is shown that tensile triangular lattice materials can belong to every class of symmetry but owns a Cauchy elasticity, that flexural ones

are at least tetragonal and that combined ones can belong to any symmetry class. It is also shown that auxeticity (for isotropic materials) requires the flexural part to be predominant. An interesting case of non trivial isotropy (with a non-D_3 microstructure) with a weak line which orientates the crack is detailed. One may think about industrial applications for example for packaging (with a preferred direction for fracture) or for crash engineering.

The engineering problem consists in findind the lattice properties given the desired stiffness tensor of the homogenized material. Unfortunately the obtained formulas are not always or not easily invertible thus the design process still requires a computer-aided procedure. However this procedure is obviously much simpler than finding the five (or eight) material's properties with respect to the six components of the stiffness tensor thanks to an numerical FEM homogenization method.

This work can be extended to other types of 2D lattices, to 3D and to richer kinematics such as Cosserat or gradient elasticities. However one would have to deal with an increasing number of invariants with the kinematics complexity. For example the gradient elasticity has eight possible symmetry classes in 2D (Auffray et al., 2009) and some hundreds invariants are nowadays required to separate the symmetry classes of a 3D stiffness tensor (Olive et al., 2017).

Appendix A. Rigidity matrix

In Eq. (7) the detailed expression of the matrix K is:

$$\mathsf{K} = \begin{bmatrix} k_a & 0 & 0 & 0 & 0 & 0 \\ 0 & 0 & -k_b \mathrm{c}_\gamma & k_b \mathrm{s}_\gamma & 0 & 0 \\ 0 & 0 & 0 & 0 & -k_c \mathrm{c}_\beta & -k_c \mathrm{s}_\beta \\ 0 & -\frac{j_a(j_b+j_c)}{aJ} & -\frac{j_a j_b \mathrm{s}_\alpha \mathrm{s}_\gamma}{aJ\mathrm{s}_\beta} & -\frac{j_a j_b \mathrm{s}_\alpha \mathrm{c}_\gamma}{aJ\mathrm{s}_\beta} & \frac{j_a j_c \mathrm{s}_\alpha \mathrm{s}_\beta}{aJ\mathrm{s}_\gamma} & -\frac{j_a j_c \mathrm{s}_\alpha \mathrm{c}_\beta}{aJ\mathrm{s}_\gamma} \\ 0 & \frac{j_a j_b}{aJ} & \frac{j_b(j_a+j_c)\mathrm{s}_\alpha \mathrm{s}_\gamma}{aJ\mathrm{s}_\beta} & \frac{j_b(j_a+j_c)\mathrm{s}_\alpha \mathrm{c}_\gamma}{aJ\mathrm{s}_\beta} & \frac{j_b j_c \mathrm{s}_\alpha \mathrm{s}_\beta}{aJ\mathrm{s}_\gamma} & -\frac{j_b j_c \mathrm{s}_\alpha \mathrm{c}_\beta}{aJ\mathrm{s}_\gamma} \\ 0 & \frac{j_a j_c}{aJ} & -\frac{j_b j_c \mathrm{s}_\alpha \mathrm{s}_\gamma}{aJ\mathrm{s}_\beta} & -\frac{j_b j_c \mathrm{s}_\alpha \mathrm{c}_\gamma}{aJ\mathrm{s}_\beta} & -\frac{j_c(j_a+j_b)\mathrm{s}_\alpha \mathrm{s}_\beta}{aJ\mathrm{s}_\gamma} & \frac{j_c(j_a+j_b)\mathrm{s}_\alpha \mathrm{c}_\beta}{aJ\mathrm{s}_\gamma} \end{bmatrix} \tag{A.1}$$

and the value of the angle of rotation of the nodes is:

$$\theta = \frac{j_a}{aJ} u_{\mathrm{BC2}} - \frac{j_b \mathrm{s}_\alpha \mathrm{s}_\gamma}{aJ\mathrm{s}_\beta} u_{\mathrm{CA1}} - \frac{j_b \mathrm{s}_\alpha \mathrm{c}_\gamma}{aJ\mathrm{s}_\beta} u_{\mathrm{CA2}} + \frac{j_c \mathrm{s}_\alpha \mathrm{s}_\beta}{aJ\mathrm{s}_\gamma} u_{\mathrm{AB1}} - \frac{j_c \mathrm{s}_\alpha \mathrm{c}_\beta}{aJ\mathrm{s}_\gamma} u_{\mathrm{AB2}} \tag{A.2}$$

where $J = j_a + j_b + j_c$.

Appendix B. Noticeable relations

We list here some remarkable relations which links the tensile $\mathbb{C}^{\mathrm{t}}$ and flexural $\mathbb{C}^{\mathrm{f}}$ stiffness tensor components or invariants to the lattice material geometrical $(S, \alpha, \beta, \gamma)$ and mechanical $(k_a, k_b, k_c, j_a, j_b, j_c)$ characteristics.

For the tensile material the change of variables:

$$k'_a = k_a \frac{\mathrm{s}_\alpha}{\mathrm{s}_\beta \mathrm{s}_\gamma}, \quad k'_b = k_b \frac{\mathrm{s}_\beta}{\mathrm{s}_\alpha \mathrm{s}_\gamma}, \quad k'_c = k_c \frac{\mathrm{s}_\gamma}{\mathrm{s}_\alpha \mathrm{s}_\beta} \tag{B.1}$$

allows one to find five linear relations:

$$\begin{bmatrix} 8I_1 \\ \sqrt{2}(\bar{C}^{\mathrm{t}}_{13}+\bar{C}^{\mathrm{t}}_{23}) \\ \bar{C}^{\mathrm{t}}_{11}-\bar{C}^{\mathrm{t}}_{22} \\ 2\sqrt{2}(\bar{C}^{\mathrm{t}}_{13}-\bar{C}^{\mathrm{t}}_{23}) \\ \bar{C}^{\mathrm{t}}_{11}+\bar{C}^{\mathrm{t}}_{22}-6\bar{C}^{\mathrm{t}}_{12} \end{bmatrix} = \begin{bmatrix} 1 & 1 & 1 \\ 0 & -\mathrm{s}_{2\gamma} & \mathrm{s}_{2\beta} \\ 1 & \mathrm{c}_{2\gamma} & \mathrm{c}_{2\beta} \\ 0 & -\mathrm{s}_{4\gamma} & \mathrm{s}_{4\beta} \\ 1 & \mathrm{c}_{4\gamma} & \mathrm{c}_{4\beta} \end{bmatrix} \cdot \begin{bmatrix} k'_a \\ k'_b \\ k'_c \end{bmatrix} \tag{B.2}$$

in which I_1 is the first invariant (29) which is equal to I_2 in this case. The third and fourth invariants are given by the following quadratic forms:

$$2I_3 = \begin{bmatrix} k'_a \\ k'_b \\ k'_c \end{bmatrix}^T \cdot \begin{bmatrix} 1 & \mathrm{c}_{2\gamma} & \mathrm{c}_{2\beta} \\ \mathrm{c}_{2\gamma} & 1 & \mathrm{c}_{2\alpha} \\ \mathrm{c}_{2\beta} & \mathrm{c}_{2\alpha} & 1 \end{bmatrix} \cdot \begin{bmatrix} k'_a \\ k'_b \\ k'_c \end{bmatrix} \tag{B.3}$$

$$8I_4 = \begin{bmatrix} k'_a \\ k'_b \\ k'_c \end{bmatrix}^T \cdot \begin{bmatrix} 1 & \mathrm{c}_{4\gamma} & \mathrm{c}_{4\beta} \\ \mathrm{c}_{4\gamma} & 1 & \mathrm{c}_{4\alpha} \\ \mathrm{c}_{4\beta} & \mathrm{c}_{4\alpha} & 1 \end{bmatrix} \cdot \begin{bmatrix} k'_a \\ k'_b \\ k'_c \end{bmatrix} \tag{B.4}$$

For the flexural material one finds an interesting linear relation:

$$2\bar{C}^{\mathrm{f}}_{11}+\bar{C}^{\mathrm{f}}_{33} = \frac{1}{JS} \begin{bmatrix} 1-\mathrm{c}_{2\alpha} \\ 1-\mathrm{c}_{2\beta} \\ 1-\mathrm{c}_{2\gamma} \end{bmatrix}^T \cdot \begin{bmatrix} j_b j_c \\ j_c j_a \\ j_a j_b \end{bmatrix} \tag{B.5}$$

and a quadratic one:

$$\bar{C}^{\mathrm{f}}_{11}\bar{C}^{\mathrm{f}}_{33}-\bar{C}^{\mathrm{f}}_{13}\bar{C}^{\mathrm{f}}_{13} = \frac{\mathrm{s}^2_\alpha \mathrm{s}^2_\beta \mathrm{s}^2_\gamma}{J^2S^2} \begin{bmatrix} j_b j_c \\ j_c j_a \\ j_a j_b \end{bmatrix}^T \cdot \begin{bmatrix} 0 & 1 & 1 \\ 1 & 0 & 1 \\ 1 & 1 & 0 \end{bmatrix} \cdot \begin{bmatrix} j_b j_c \\ j_c j_a \\ j_a j_b \end{bmatrix} \tag{B.6}$$

Acknowledgments

Funding: This work has been realized during the MatSyMat project funded by the Région des Pays de la Loire and granted by the Pôle EMC2.

Authors thank Alexandra Reynolds for her help with the English language.

References

Auffray, N., 2008. Démonstration du théorème d'Hermann à partir de la méthode ForteVianello. Comptes Rendus Mécanique 336 (5), 458 – 463.
URL http://www.sciencedirect.com/science/article/pii/S1631072108000302

Auffray, N., february 2017. Géométrie des espaces de tenseurs, application à l'élasticité anisotrope classique et généralisée. Habilitation à diriger des recherches, Université Paris Est.

Auffray, N., Bouchet, R., Bréchet, Y., 2009. Derivation of anisotropic matrix for bi-dimensional strain-gradient elasticity behavior. International Journal of Solids and Structures 46 (2), 440 – 454.
URL http://www.sciencedirect.com/science/article/pii/S0020768308003624

Auffray, N., Ropars, P., 2016. Invariant-based reconstruction of bidimensional elasticity tensors. International Journal of Solids and Structures 87, 183–193.

Bechterew, P., 1926. Analytical study of the generalized Hookes law. application of the method of coordinate transformation. Zh. Russ. Fiz.-Khim. Obshch. Leningrad. Univ., Fizika 58, 415–446.

Blinowski, A., Ostrowska-Maciejewska, J., Rychlewski, J., 1996. Two-dimensionnal hooke's tensors - isotropic decomposition, effective symmetry criteria. Arch. Mech. 48 (2), 325–345.

Born, M., Huang, K., 1954. Dynamical theory of the crystal lattices. Clarendon press.

Bornert, M., Bretheau, T., Gilormini, P., 2002. Homogénéisation en mécanique des matériaux 1 : matériaux aléatoires élastiques et milieux périodiques. Mécanique et ingénierie des matériaux. Hermes.

Cauchy, L. A., 1913. Oeuvres complètes, 2ème série. Gauthier-Villars.

Chevalier, L., Konieczka, S., 2000. Liaisons élastiques : calculs et applications. Technologie 108, 35–42.

De Saxcé, G., Vallée, C., 2013. Invariant measures of the lack of symmetry with respect to the symmetry groups of 2D elasticity tensors. Journal of Elasticity 111 (1), 21–39.

Dirrenberger, J., Forest, S., Jeulin, D., 2013. Effective elastic properties of auxetic microstructures: anisotropy and structural applications. International Journal of Mechanics and Materials in Design 9, 21–33.

Dos Reis, F., Ganghoffer, J., 2012. Construction of micropolar continua from the asymptotic homogenization of beam lattices. Computers & Structures 112113, 354 – 363.
URL http://www.sciencedirect.com/science/article/pii/S0045794912001940

399 Duy-Khanh, T., 2011. Méthodes d'homogénéisation d'ordre supérieur pour
400 les matériaux architecturés. Ph.D. thesis, école Nationale Supérieure des
401 Mines de Paris.

402 Fleck, N. A., Deshpande, V. S., Ashby, M. F., 2010. Micro-architectured
403 materials: past, present and future. Proceedings of the Royal Society of
404 London A: Mathematical, Physical and Engineering Sciences 466 (2121),
405 2495–2516.
406 URL http://rspa.royalsocietypublishing.org/content/466/2121/2495

407 Forte, S., Vianello, M., 1996. Symmetry classes for elasticity tensors. Journal
408 of Elasticity 43 (2), 81–108.
409 URL http://dx.doi.org/10.1007/BF00042505

410 Forte, S., Vianello, M., 2014. A unified approach to invariants of plane elas-
411 ticity tensors. Meccanica 49 (9), 2001–2012.
412 URL http://dx.doi.org/10.1007/s11012-014-9916-y

413 François, M., Geymonat, G., Berthaud, Y., 1998. Determination of the
414 symmetries of an experimentally determined stiffness tensor: Application
415 to acoustic measurements. International Journal of Solids and Structures
416 35 (31), 4091 – 4106.
417 URL http://www.sciencedirect.com/science/article/pii/S002076839700303X

418 Jibawy, A., Julien, C., Desmorat, B., Vincenti, A., Léné, F., 2011. Hierarchi-
419 cal structural optimization of laminated plates using polar representation.
420 International Journal of Solids and Structures 48 (18), 2576 – 2584.
421 URL http://www.sciencedirect.com/science/article/pii/S0020768311001879

Kelvin (Thomson), W., 1856. Elements of mathematical theory of elasticity. Phil. Trans. R. Soc. 146, 481–498.

Kelvin (Thomson), W., 1893. On the elasticity of a crystal according to Boscovich. Proceedings of the Royal Society of London 54, 59–75.

Lakes, R., 1986. Experimental microelasticity of two porous solids. International Journal of Solids and Structures 22 (1), 55 – 63.
URL http://www.sciencedirect.com/science/article/pii/0020768386901034

Le Dret, H., Raoult, A., 2011. Homogenization of hexagonal lattices. Comptes Rendus Mathematique 349 (1), 111 – 114.
URL http://www.sciencedirect.com/science/article/pii/S1631073X10003912

Milton, G. W., 1992. Composite materials with poisson's ratios close to 1. Journal of the Mechanics and Physics of Solids 40 (5), 1105 – 1137.
URL http://www.sciencedirect.com/science/article/pii/0022509692900638

Milton, G. W., 2002. The theory of composites. Cambridge University Press.

Olive, M., Kolev, B., Auffray, N., 2017. A minimal integrity basis for the elasticity tensor. Archive for Rational Mechanics and Analysis.
URL https://hal.archives-ouvertes.fr/hal-01467996

Perrin, D., 2013. Le plus grand angle fait face au plus grand côté.
URL https://www.math.u-psud.fr/ perrin/SurGeometrie/Grandangle.pdf

Réthoré, J., Kaltenbrunner, C., Dang, T. B. T., Chaudet, P., Kuhn, M., 2015. Gradient-elasticity for honeycomb materials: Validation and identification from full-field measurements. International Journal of Solids

and Structures 72, 108 – 117.
URL http://www.sciencedirect.com/science/article/pii/S0020768315003212

Rothenburg, L., Berlin, A. A., Bathurst, R. J., 1991. Microstructure of isotropic materials with negative poisson's ratio. Nature 354, 470–472.

Rychlewski, J., 1984. On hooke's law. Journal of Applied Mathematics and Mechanics 48 (3), 303 – 314.
URL http://www.sciencedirect.com/science/article/pii/0021892884901370

Vannucci, P., 2002. A special planar orthotropic material. Journal of elasticity and the physical science of solids 67 (2), 81–96.
URL http://dx.doi.org/10.1023/A:1023949729395

Vannucci, P., Desmorat, B., 2016. Plane anisotropic rari-constant materials. Mathematical Methods in the Applied Sciences 39 (12), 3271–3281, mma.3770.
URL http://dx.doi.org/10.1002/mma.3770

Verchery, G., 1982. Les Invariants des Tenseurs d'Ordre 4 du Type de l'Élasticité. Springer Netherlands, Dordrecht, pp. 93–104.

Vianello, M., 1997. An integrity basis for plane elasticity tensors. Arch. Mech. 49 (1), 198–208.

Wadhawan, V., 1987. The generalized Curie principle, the Hermann theorem, and the symmetry of macroscopic tensor properties of composites. Materials Research Bulletin 22 (5), 651 – 660.
URL http://www.sciencedirect.com/science/article/pii/0025540887901140

466 Walpole, L., 1984. Fourth-rank tensors of the thirty-two crystal classes: Mul-
467 tiplication tables. Proceedings of the Royal Society 58, 149–179.